BIOCHEMISTRY
including biophysical chemistry & molecular biology

Article

pubs.acs.org/biochemistry

Kinetic Analysis of Human PrimPol DNA Polymerase Activity Reveals a Generally Error-Prone Enzyme Capable of Accurately Bypassing 7,8-Dihydro-8-oxo-2′-deoxyguanosine

Maroof K. Zafar,[†] Amit Ketkar,[†] Maria F. Lodeiro,[‡] Craig E. Cameron,[‡] and Robert L. Eoff*[,†]

[†]Department of Biochemistry and Molecular Biology, University of Arkansas for Medical Sciences, Little Rock, Arkansas 72205-7199, United States

[‡]Department of Biochemistry and Molecular Biology, Pennsylvania State University, 201 Althouse Laboratory, University Park, Pennsylvania 16802, United States

Supporting Information

ABSTRACT: Recent studies have identified human PrimPol as a new RNA/DNA primase and translesion DNA synthesis polymerase (TLS pol) that contributes to nuclear and mitochondrial DNA replication. We investigated the mechanism of PrimPol polymerase activity on both undamaged and damaged DNA substrates. With Mg^{2+} as a cofactor, PrimPol binds primer-template DNA with low affinity $K_{d,DNA}$ values (~200−1200 nM). DNA binding is enhanced 34-fold by Mn^{2+} ($K_{d,DNA}$ = 27 nM). The pol activity of PrimPol is increased 400−1000-fold by Mn^{2+} compared to Mg^{2+} based on steady-state kinetic parameters. PrimPol makes a mistake copying undamaged DNA once every ~100−2500 insertions events, which is comparable to other TLS pols, and the fidelity of PrimPol is ~1.7-fold more accurate when Mg^{2+} is the cofactor compared to Mn^{2+}. PrimPol inserts dCMP opposite 8-oxo-dG with 2- (Mn^{2+}) to 6-fold (Mg^{2+}) greater efficiency than dAMP misinsertion. PrimPol-catalyzed dCMP insertion opposite 8-oxo-dG proceeds at ~25% efficiency relative to unmodified template dG, and PrimPol readily extends from dC:8-oxo-dG base pairs (bps) with ~2-fold greater efficiency than dA:8-oxo-dG bps. A tetrahydrofuran (THF) abasic-site mimic decreases PrimPol activity to ~0.04%. In summary, PrimPol exhibits the fidelity typical of other TLS pols, is rather unusual in the degree of activation afforded by Mn^{2+}, and accurately bypasses 8-oxo-dG, a DNA lesion of special relevance to mitochondrial DNA replication and transcription.

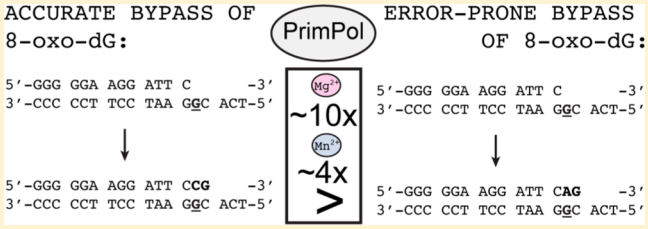

DNA replication requires the coordinated action of many different proteins and enzymes.[1−3] Decades of research into the mechanisms of genomic maintenance have provided us with a wealth of knowledge regarding the molecular transactions that occur at sites of DNA synthesis. However, new features of the replisome are still being discovered, and our view of the replication machinery is continually being refined. One such addition to models for eukaryotic replication is found in the newly described bifunctional enzyme human PrimPol.[4,5]

PrimPol is a 560 a.a. protein encoded by the human gene *CCDC111* that was recently shown to possess both RNA/DNA primase and DNA polymerase (pol) activities.[4−6] PrimPol is the second member of the archaeal-eukaryotic primase (AEP) superfamily member to be identified in humans, with the Pol-α-associated DNA primase subunit, Prim1 (also called p48), being the other.[7,8] In addition to primase and pol catalytic activities, PrimPol also possesses a UL52-like zinc finger domain that regulates primase processivity and may affect some aspects of pol fidelity.[9] PrimPol prefers to synthesize DNA primers *de novo* as opposed to RNA primers, and it has been proposed that PrimPol acts to reinitiate DNA synthesis downstream from lesions that block the replication machinery.[10] Consistent with a role for PrimPol in DNA damage tolerance, it is found localized to chromatin during DNA replication and becomes enriched following exposure to DNA damaging agents (e.g., UV irradiation). Further study revealed that PrimPol interacts with RPA and can bypass some DNA adducts with relative ease,[4,5,10,11] leading to the proposal that PrimPol is a new translesion DNA synthesis pol (TLS pol).

PrimPol is found localized to both the nucleus and in mitochondria,[4] in line with an earlier study that isolated mitochondrial primase activity from human cells without identifying the gene product responsible for the primase action.[12] The reported role for PrimPol in maintenance of mitochondrial DNA (mtDNA) is especially intriguing since DNA pol gamma (hpol γ) has been considered to be the only enzyme able to perform DNA synthesis in mammalian mitochondria. A model in which hpol γ is the sole enzyme capable of performing synthesis on damaged mtDNA presents a problem when one considers two very basic ideas related to mtDNA damage: (1) mitochondrial DNA is subject to higher levels of oxidative damage than nuclear DNA, and (2) hpol γ is not proficient at bypassing even the simplest of oxidative

Received: August 15, 2014
Revised: September 24, 2014
Published: September 25, 2014

   dx.doi.org/10.1021/bi501024u | *Biochemistry* 2014, 53, 6584−6594

Table 1. DNA Substrates Used in the Study

Substrates used in DNA binding studies:

```
Substrate 1 (13/18-mer):
5′-(FAM) TTT GGG GGA AGG ATT C-3′
          3′-CCC CCT TCC TAA GGC ACT-5′
Substrate 2 (13/28-mer):
5′-(FAM) TTT GGG GGA AGG ATT C-3′
          3′-CCC CCT TCC TAA GGC ACT GCA CTA CGC T-5′
Substrate 3 (24/29-mer):
5′-(FAM) TTT GCC TCG AGC CAG CCG CAG ACG CAC-3′
          3′-CGG AGC TCG GTC GGC GTC TGC GTG GAT CC -5′
Substrate 4 (24/39-mer):
5′-(FAM) TTT GCC TCG AGC CAG CCG CAG ACG CAC-3′
          3′-CGG AGC TCG GTC GGC GTC TGC GTG GAT CCT GCG GCT GCT -5′
```

Substrates used in DNA Pol Activity Assays:

```
[a]Substrate 5 (13/18G-mer):
5′-(FAM) TTT GGG GGA AGG ATT C-3′
          3′-CCC CCT TCC TAA GGC ACT-5′
Substrate 6 (13/18T-mer):
5′-(FAM) TTT GGG GGA AGG ATT C-3′
          3′-CCC CCT TCC TAA GTC ACT-5′
Substrate 7 (13/18A-mer):
5′-(FAM) TTT GGG GGA AGG ATT C-3′
          3′-CCC CCT TCC TAA GAC ACT-5′
Substrate 8 (13/18C-mer):
5′-(FAM) TTT GGG GGA AGG ATT C-3′
          3′-CCC CCT TCC TAA GCT ACT-5′
Substrate 9 (13/18-mer):
5′-(FAM) TTT GGG GGA AGG ATT C-3′
          3′-CCC CCT TCC TAA G 8-oxo-dG C ACT-5′
[b]Substrate 10 (13/18-mer):
5′-(FAM) TTT GGG GGA AGG ATT C-3′
          3′-CCC CCT TCC TAA G AP C ACT-5′
Substrate 11 (14C/18-mer):
5′-(FAM) TTT GGG GGA AGG ATT CC-3′
          3′-CCC CCT TCC TAA GGC ACT-5′
Substrate 12 (14A/18-mer):
5′-(FAM) TTT GGG GGA AGG ATT CA-3′
          3′-CCC CCT TCC TAA GGC ACT-5′
Substrate 13 (14C/18-mer):
5′-(FAM) TTT GGG GGA AGG ATT C    C-3′
          3′-CCC CCT TCC TAA G 8-oxo-dG C ACT-5′
Substrate 14 (14A/18-mer):
5′-(FAM) TTT GGG GGA AGG ATT C    A-3′
          3′-CCC CCT TCC TAA G 8-oxo-dG C ACT-5′
```

[a]The template base paired with the incoming dNTP is underlined. [b]AP = THF abasic site.

lesions, such as 7,8-dihydro-8-oxo-2′-deoxyguanosine (8-oxo-dG). In the nucleus, blocks to replication fork progression can activate replication stress response pathways that recruit DNA repair and damage tolerance proteins/enzymes to sites of fork stalling.[13,14] There are DNA repair mechanisms at work in mitochondria, primarily in the form of base excision repair (BER), but given the amount of damage ubiquitous to mtDNA, there are likely to be numerous encounters between the mitochondrial replication/transcription machineries and DNA adducts. The mechanism by which damage to mtDNA is tolerated in the absence of repair has been a long-standing question in the field of mtDNA replication, and the emergence of PrimPol as a potential means of performing TLS in mitochondria has opened up a number of fascinating possibilities.

While a flurry of studies have shown that PrimPol can bypass DNA adducts and that it likely contributes to TLS in cells, a detailed quantitative analysis of PrimPol DNA binding and enzymatic activity is largely absent. We have performed steady-state kinetic analysis of PrimPol DNA polymerase activity so that comparisons can be made between this purported TLS enzyme and other well-studied TLS pols. We find that PrimPol exhibits weak binding affinity to primer-template DNA (p/t-DNA) in the presence of Mg^{2+}, but this affinity is dramatically increased by Mn^{2+}. The kinetic parameters for nucleotide incorporation suggest that PrimPol is highly stimulated by Mn^{2+} and has a misinsertion frequency on par with other TLS pols, such as the Y-family pols. Finally, we quantified the efficiency and accuracy of PrimPol activity on damaged DNA templates and find that PrimPol preferentially bypasses 8-oxo-dG in an accurate manner. In short, our results provide the first quantitative insights into the PrimPol mechanism of action as a TLS pol and lay the groundwork for more detailed kinetic study of individual steps within the PrimPol catalytic cycle.

MATERIALS AND METHODS

Materials. All chemicals were molecular biology grade or better. 2′-Deoxynucleoside triphosphates (dNTPs) were obtained from Promega (Madison, WI). All oligonucleotides used in this work (with the exception of tetrahydrofuran, THF-containing oligonucleotides) were synthesized by Integrated DNA Technologies (Coralville, IA) and purified using high-

dx.doi.org/10.1021/bi501024u | Biochemistry 2014, 53, 6584−6594

performance liquid chromatography by the manufacturer, with analysis by matrix-assisted laser desorption time-of-flight mass spectrometry. Oligonucleotides containing THF were synthesized by Midland Certified Reagent Co. (Midland, TX). Primers were labeled at the 5′-end with 6-carboxyfluorescein (FAM). Fourteen different primer-template DNA (p/t-DNA) substrates were used in the study (Table 1).

Expression and Purification of Recombinant Human PrimPol. Rosetta (DE3) competent *Escherichia coli* cells were transformed with 10 ng of pSUMO-PrimPol (WT or AA), plated onto agar media containing the appropriate antibiotics, and grown at 30 °C overnight. The pSUMO vector was obtained from LifeSensors, Inc. Then 2 × 100 mL (starter cultures) NZCYM media containing kanamycin (25 μg/mL, K25) and chloramphenicol (20 μg/mL, C20) were inoculated with a smear of colonies from freshly plated and transformed cells. These cultures were grown at 37 °C with shaking (250 rpm) to an OD_{600} of 1.0. Next, 4 × 500 mL autoinducing media (Amresco) containing K75 and C60 (3 times) was inoculated to an OD_{600} of 0.025 with the starter culture and grown at 37 °C with shaking (250 rpm) to an OD_{600} of 1.0. Once the cultures reached OD_{600} of 1.0, they were placed at 4 °C until the temperature reached 15 °C. One milliliter of culture was removed for uninduced sample. The flasks were then grown at 15 °C with shaking (250 rpm) overnight for 40 h. A 1 mL aliquot of culture was removed for induced sample after 40 h to check for protein expression. After verifying induction, cells were harvested by centrifugation, washed once with cold $T_{10}E_1$ (20 mL/L OD), centrifuged again, and frozen at −80 °C (T10 E1 is 10 mM Tris pH 8 and 1 mM EDTA).

For the purification, frozen cell pellets were thawed on ice and suspended in 50 mM Tris (pH 8.0) buffer containing 500 mM NaCl, 10 mM β-mercaptoethanol (β-ME), 20% (v/v) glycerol, 1.4 μg/mL pepstatin A, and 1 μg/mL leupeptin (Buffer A) at a concentration of 5 mL of lysis buffer per 1 g of cell pellet. A single EDTA-free protease tablet (Roche) was added per 10 g of cell pellet. Cells were lysed by passing through a French pressure cell at 20 000 psi. Phenylmethylsulfonyl fluoride (PMSF) and nonidet P-40 (NP-40) were added immediately after lysis to final concentrations of 1 mM and 0.1% (v/v), respectively. The lysate was centrifuged for 30 min at 25 000 rpm (75000*g*) at 4 °C using a Beckman JA 30.50 rotor. The clarified lysate was decanted and then loaded onto a Ni-NTA column at a flow rate of 0.5 mL/min (approximately 1 mL of bed volume/30 mg of total protein). After the clarified lysate was loaded, the column was washed at a flow rate of 1 mL/min with 20 column volumes of 50 mM Tris (pH 8.0) buffer containing 500 mM NaCl, 10 mM β-ME, 20% (v/v) glycerol containing 5 mM imidazole and 0.1% (v/v) NP40 (Buffer B). Protease inhibitor pepstatin, leupeptin, and PMSF were present in all the buffers at the indicated concentrations above. The column was washed a second time with 10 column volumes of buffer B containing 5 mM imidazole (NP40 was left out of all subsequent buffers) and then with 5 column volumes of buffer B containing 50 mM imidazole. The protein was then eluted with buffer B containing 500 mM imidazole and collected in one column volume fractions and assayed for purity by SDS-PAGE. In addition, all fractions were run on 1% (w/v) agarose gel to check for nucleic acid contamination. Fractions were pooled based upon purity. Pepstatin A and leupeptin (1 μg/mL final) were added to the pooled samples along with PMSF (1 mM final) prior to adding Ulp1 and dialyzing overnight. To cleave the SUMO-PrimPol fusion protein, Ulp1 protease (LifeSensors Inc.) (10 units per 1 mg of SUMO fusion) was added to the pooled sample, and dialysis was performed overnight at 4 °C against two changes of 1 L of 20 mM HEPES (pH 7.5) buffer containing 500 mM NaCl, 10 mM β-ME, 20% (v/v) glycerol (Buffer C) (12−14 000 Da MWCO membrane). After 16 h of incubation, the cleavage of the SUMO fusion protein was verified by SDS-PAGE, and the dialyzed sample was loaded onto a second Ni-NTA column equilibrated with Buffer C at a flow rate of 1 mL/min (approximately 1 mL of bed volume/5 mg of total protein). After loading, the column was washed at a flow rate of 1 mL/min with 10 column volumes of Buffer C. The pass-through and 10 one-half column volume fractions were collected and assayed for purity by SDS-PAGE. Fractions were pooled based upon purity and concentration.

The pooled sample was then concentrated to ∼4 mg/mL final with the Vivaspin protein concentrators and further purified in a gel filtration column Superdex 75 in 20 mM HEPES (pH 7.5) buffer containing 500 mM NaCl, 20% (v/v) glycerol, 1 mM dithiothreitol (DTT). Fractions of 3 mL were collected and after Bradford and PAGE analysis fractions containing the proteins were pooled. Pooled PrimPol was concentrated with the Vivaspin protein concentrator. The protein concentration was determined and supplemented with 1 mM tris(2-carboxyethyl)phosphine (TCEP). The protein was then aliquoted, frozen, and stored at −80 °C. The quality of the final purified protein was assessed by assaying for nuclease activity (RNase and DNase) and phosphatase activity.

Measurement of DNA Binding Affinity by Fluorescence Polarization. PrimPol DNA binding affinity was measured by incubating p/t-DNA substrates (1 nM) labeled at the 5′-end of the primer with FAM with varying concentrations of PrimPol (0 to 4 μM). Fluorescence polarization was measured in a Biotek Synergy4 plate reader using the appropriate filter sets (λ_{ex} = 485 ± 20 nm and λ_{em} = 525 ± 20 nm). All titrations were performed at 25 °C in 50 mM HEPES buffer (pH 7.5) containing 10 mM KOAc, 10 mM KCl, 0.1 mM EDTA, 2 mM β-ME, and 0.1 mg/mL bovine serum albumin (BSA). Where indicated, either 5 mM $MgCl_2$ or 5 mM $MnCl_2$ was added to the DNA binding experiment. Polarization was determined using eq 1:

$$P = \frac{(F_{\parallel} - F_{\perp})}{(F_{\parallel} + F_{\perp})} \quad (1)$$

where $F_{\parallel}$ equals fluorescence intensity parallel to the excitation plane and $F_{\perp}$ equals the fluorescence intensity perpendicular to the excitation plane. The resulting change in polarization units was plotted against protein concentration and fit to a quadratic equation to estimate the equilibrium dissociation constant for PrimPol binding to DNA ($K_{d,DNA}$).

Full-Length Extension Polymerase Assays. DNA substrates were prepared as described previously.[15] PrimPol extension reactions were initiated by adding dNTP·$MgCl_2$ (0.25 mM of each dNTP and indicated concentrations of metal ion) solution to a preincubated PrimPol·DNA complex (250 nM PrimPol and 2.5 μM DNA). All pol extension reactions were carried out at 37 °C in 10 mM HEPES buffer (pH 7.5) containing 100 mM KCl, 1 mM DTT, 100 μg mL^{-1} BSA, and 5% (v/v) glycerol. At the indicated time points, 15 μL aliquots were quenched with 85 μL of a 95% (v/v) formamide/20 mM EDTA/0.1% (w/v) bromophenol blue solution and were separated by electrophoresis on a 16% polyacryamide (w/

dx.doi.org/10.1021/bi501024u | *Biochemistry* 2014, 53, 6584−6594

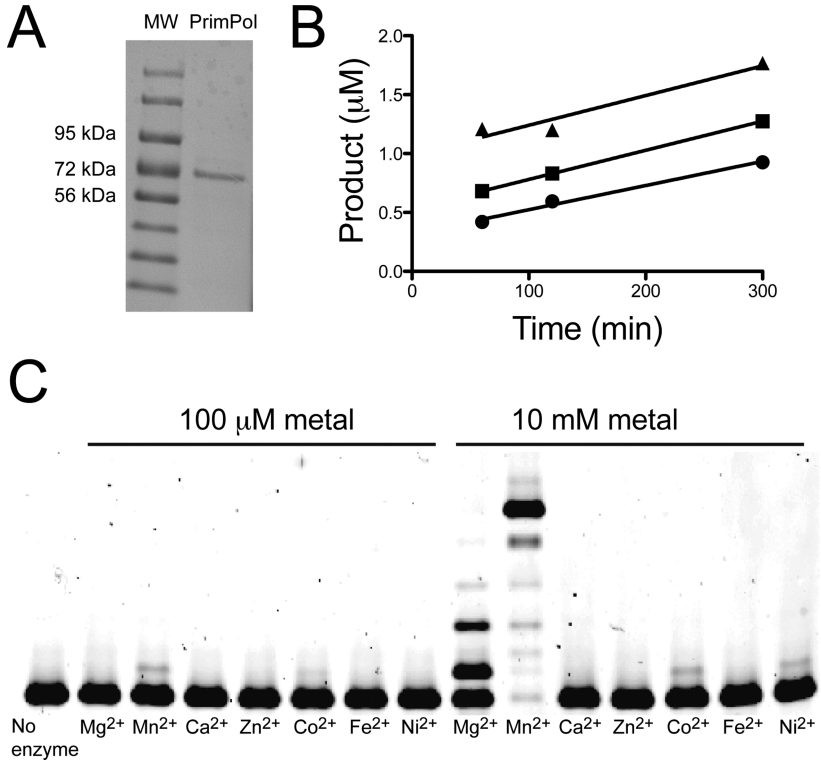

Figure 1. DNA polymerase activity of PrimPol is most strongly promoted by manganese. (A) Recombinant full-length human PrimPol (a.a. 1−560) was purified from *Escherichia coli*. (B) The polymerase activity of purified recombinant PrimPol was confirmed with an active-site titration. PrimPol (0.25 μM, ●; 0.5 μM, ■; 1 μM, ▲) was incubated with p/t-DNA (2.5 μM) and dCTP insertion was measured. Linear regression analysis resulted in a *y*-intercept of 0.32 ± 0.04, 0.53 ± 0.01, and 0.99 ± 0.13 μM for PrimPol concentrations of 0.25, 0.5 and 1 μM, respectively. (C) PrimPol (250 nM) was incubated with 13/18-mer p/t-DNA (2.5 μM), a mixture of all four dNTPs (250 μM each) and seven different metal ions at the indicated concentrations. The reactions were allowed to proceed for 30 min, and the products were separated by 16% (w/v) polyacrylamide/7 M urea gel electrophoresis. DNA synthesis is most robust with Mn^{2+} as the cofactor.

v)/7 M urea gel. The products were then visualized using a Typhoon imager (GE Healthcare Life Sciences).

Steady-State Kinetic Analysis of Polymerase Activity. Single-nucleotide incorporation by PrimPol was measured over a range of either metal or dNTP concentrations. The single-nucleotide insertion experiments were performed in a manner nearly identical to the extension reactions described above except only a single dNTP was used instead of a mixture. For reactions where the concentration of metal ion ($MgCl_2$ or $MnCl_2$) was varied, the concentration of dNTP was held constant at 2.5 mM for reactions with varying $MgCl_2$ and 100 μM for reactions with varying $MnCl_2$. Likewise, the metal ion concentration was held constant at 10 mM when the dNTP concentration was varied. The products were imaged as described for full-length extension assays and quantified using ImageQuant software (GE Healthcare Life Sciences). The initial portion of the velocity curve was fit to a linear equation in the program GraphPad Prism (GraphPad, San Diego, CA). The resulting velocity was plotted as a function of metal or dNTP concentration and then fit to a hyperbolic equation, correcting for enzyme concentration, to obtain estimates for the turnover number (k_{cat}) and Michaelis constant ($K_{M,metal}$ or $K_{M,dNTP}$). The reported steady-state parameters are derived from a single set of titration experiments. However, preliminary time course assays were used to assess the reproducibility of the experimental conditions. Additionally, the experiments measuring PrimPol-catalyzed dCMP insertion opposite template dG were repeated twice in the presence of Mn^{2+} with results that indicate very high precision.

RESULTS

Purification of Recombinant PrimPol and Metal Ion Dependence of PrimPol Polymerase Extension Activity. We purified full-length recombinant human PrimPol from *E. coli* cells (Figure 1A). An active-site titration experiment was performed to confirm the activity of the purified recombinant PrimPol (Figure 1B). We note that the majority of the previously reported pol assays were performed with PrimPol in excess of DNA substrate (often as much as 80-fold excess enzyme). Notably, we see robust polymerization by PrimPol even under enzyme limiting conditions (1:10 PrimPol/DNA, Figure 1B,C). We also reconfirmed the preference of PrimPol for Mn^{2+} over Mg^{2+} by performing pol extension assays in the presence of each metal ion cofactor (Figure 1C). As shown previously by other groups, PrimPol is more active in the presence of Mn^{2+} than it is when Mg^{2+} is the cofactor for polymerization. We then went on to test PrimPol action in the presence of other divalent metal ion cofactors. We performed pol extension assays in the presence of seven different divalent metal ions. We find that PrimPol pol activity is stimulated to a measurable extent by four different metal ions with the degree of stimulation (from greatest to least) being: Mn^{2+} > Mg^{2+} > Co^{2+} > Ni^{2+} (Figure 1C). Extension experiments with Ca^{2+}, Fe^{2+}, and Zn^{2+} failed to yield measurable product. These results confirmed the quality of our purified recombinant PrimPol and reaffirmed the preference for Mn^{2+} over other metal ion cofactors.

dx.doi.org/10.1021/bi501024u | *Biochemistry* 2014, 53, 6584−6594

Primer-Template DNA Binding Properties. Next, we wanted to determine the substrate binding preference for PrimPol. It was previously shown that PrimPol could bind single-stranded DNA (ssDNA), as well as blunt-ended DNA using gel shift assays.[9] Binding to ssDNA and blunt-end DNA was only observed at concentrations of PrimPol higher than 500 nM, which indicates relatively weak binding affinity compared to other pols. Strangely enough, no binding studies have been reported for primer-template DNA (p/t-DNA) even though PrimPol performs DNA synthesis on these types of substrates. Therefore, we performed DNA binding experiments with p/t-DNA substrates of varying lengths.

Fluorescence anisotropy was used to measure equilibrium dissociation constants defining PrimPol binding to different p/t-DNA substrates (Table 1). First, we measured PrimPol binding to a short 13/18-mer p/t-DNA substrate, which has a five nucleotide (nt) ssDNA overhang on the template strand. In a buffer solution that contains Mg^{2+} as the metal ion cofactor, PrimPol binds this short 13/18-mer p/t-DNA substrate with a $K_{d,DNA}$ of 910 (±550) nM (Table 2). Substituting Mg^{2+} with Mn^{2+} dramatically decreased the $K_{d,DNA}$ for PrimPol binding to the 13/18-mer to 27 (±8) nM (Table 2). In addition to the p/t-DNA substrates, binding of PrimPol to 24-mer ssDNA was also examined (Table S1). PrimPol exhibited very weak affinity for ssDNA in the presence of Mg^{2+} ($K_{d,DNA}$ = 4500 ± 2500 nM). The affinity of PrimPol for ssDNA is increased ~7-fold by Mn^{2+} ($K_{d,DNA}$ = 670 ± 180 nM), which is not as dramatic of a change as that observed for p/t-DNA. Changing the metal ion in the binding solution from Mg^{2+} to Mn^{2+} results in ~34-fold tighter binding to 13/18-mer p/t-DNA, consistent with the dramatic increase in pol activity observed for this substrate with Mn^{2+}.

Table 2. Equilibrium Dissociation Constants for PrimPol Binding to p/t-DNA

substrate	metal	$K_{d,DNA}$ (nM)[a]
1 (13/18-mer)	Mg^{2+}	910 ± 550
	Mn^{2+}	27 ± 8
2 (13/28-mer)	Mg^{2+}	240 ± 100
3 (24/29-mer)	Mg^{2+}	1200 ± 550
4 (24/39-mer)	Mg^{2+}	350 ± 160

[a]The binding data were fit to a quadratic equation. The values reported represent the mean ± s.e.m. (n = 2).

We went on to measure PrimPol binding to a p/t-DNA substrate that possessed a longer ssDNA overhang in the template strand (substrate 2, 13/28-mer). In the presence of Mg^{2+}, increasing the length of the ssDNA portion of the p/t-DNA from 5 to 15 nts increased the apparent affinity of PrimPol for p/t-DNA, as evidenced by a lower $K_{d,DNA}$ of 240 (±140) nM for substrate 2 (Table 2). We then tested PrimPol binding to a pair of p/t-DNA substrates with a longer 24 bp dsDNA region (substrates 3 and 4). In Mg^{2+}, PrimPol binding to the 24/29-mer (substrate 3), which possesses a five nt ssDNA overhang, was weak, with a $K_{d,DNA}$ value of 1210 (±550) nM. PrimPol was found to bind the 24/39-mer, which possesses a 15 nt ssDNA overhang, with higher affinity ($K_{d,DNA}$ = 350 ± 160 nM). From these results, we conclude that increasing the ssDNA overhang of p/t-DNA substrates results in tighter binding, while the length of the dsDNA region has little effect on the affinity of the enzyme for the DNA substrate.

Stimulation of PrimPol Catalytic Efficiency by Mn^{2+}. Next, we wanted to quantify the metal ion-dependent changes in PrimPol catalytic efficiency. Based on our pol extension results, we were interested in determining the magnitude of PrimPol stimulation by Mn^{2+} relative to Mg^{2+}. We varied the concentration of metal in the reaction mixture and measured PrimPol-catalyzed insertion of dCMP opposite template dG (substrate 1) at saturating concentrations of nucleotide. Steady-state kinetic analysis reveals that the turnover number (k_{cat}) for PrimPol catalysis is increased ~30-fold by Mn^{2+} compared to Mg^{2+} (Table 3). Using the specificity constant (k_{cat}/K_M) as a measure of PrimPol catalytic efficiency, it would appear that PrimPol has a ~16-fold preference for Mn^{2+} over Mg^{2+} (Table 3).

Table 3. Steady-State Kinetic Analysis of Metal-Ion-Dependent Nucleotidyl Transfer by PrimPol

metal[a]	k_{cat} (min^{-1})	$K_{m,metal}$ (mM)	$k_{cat}/K_{m,metal}$ (min^{-1} mM^{-1})
magnesium	0.23 ± 0.004	1.2 ± 0.1	0.20
manganese	7.0 ± 0.2	2.2 ± 0.2	3.1

[a]Pol assays were performed on a 13/18mer primer-template (substrate 1) with dCTP as the incoming nucleotide triphosphate and dG as the template base. For determination of kinetic values, graphs of product formation versus dNTP concentration were plotted using nonlinear regression analysis (one-site hyperbolic fit) in the GraphPad prism program. The standard error of the fit is reported for each value.

Then we determined the effect of the metal ion cofactor on the kinetics of nucleotide selectivity by PrimPol. Measuring insertion of dCMP opposite template dG, we find that substituting Mn^{2+} increases the k_{cat} ~18-fold relative to Mg^{2+} (Table 4). Remarkably, the specificity constant for dCMP insertion across from template dG is increased over 400-fold when saturating concentrations of Mn^{2+} and Mg^{2+} are compared (Table 4). The large increase in the specificity constant is from the 18-fold increase in the k_{cat} combined with an approximate 25-fold decrease in the $K_{m,dNTP}$ when Mn^{2+} is the cofactor. The $K_{M,dNTP}$ values measured for PrimPol in the presence of Mg^{2+} are extraordinarily high (in the hundreds of micromolar) for correct insertion events. In the presence of Mn^{2+} the measured $K_{M,dNTP}$ values for accurate copying of undamaged DNA are closer to physiologically relevant concentrations (in the tens of micromolar). Thus, Mn^{2+} could serve as something of a "switch" that activates PrimPol-catalyzed nucleotide insertion by increasing the affinity of the enzyme for DNA, as well as the efficiency of pol activity.

Measurement of PrimPol Catalytic Efficiency and Misinsertion Frequency on Undamaged DNA Templates. A fundamental parameter for every DNA pol is the rate at which the enzyme makes mistakes (i.e., misinserts non-Watson−Crick bps). The misinsertion frequency (f_{ins}) for a pol is often reported as the efficiency of incorrect bp formation divided by the efficiency of Watson−Crick bp formation. Many TLS pols have error-rates on the order of 1 mistake every few hundred (f_{ins} = 0.01) to few thousand (f_{ins} = 0.001) catalytic events, with some enzymes like hpol ι exhibiting misinsertion frequencies greater than 1 (i.e., non-Watson−Crick bps are preferred over Watson−Crick bps).

Given its purported role in DNA damage tolerance, we wanted to determine the misinsertion frequency of PrimPol on both undamaged and damaged DNA templates. To do so, we first measured the catalytic efficiency of PrimPol in inserting the

dx.doi.org/10.1021/bi501024u | Biochemistry 2014, 53, 6584−6594

Table 4. Steady-State Kinetic Comparison of PrimPol Fidelity Across from Template dG in the Presence of Magnesium and Manganese

template	Metal	dNTP	Base	k_{cat} (min^{-1})	K_m (mM)	k_{cat}/K_m (min^{-1} mM^{-1})	f_{ins}[a] (misinsertion frequency)
dG	Mg^{2+}	dCTP		0.54 ± 0.05	0.84 ± 0.25	0.64	
		dGTP		0.0014 ± 0.0001	0.36 ± 0.10	0.0039	0.006
dG	Mn^{2+}	dCTP[b]		10.8 ± 1.3	0.036 ± 0.004	300	
		dGTP		0.072 ± 0.002	0.023 ± 0.003	3.1	0.01

[a]The frequencies of misinsertion were calculated relative to insertion of dCTP opposite dG using the ratio $(k_{cat}/K_{M,mispaired\ dNTP})/(k_{cat}/K_{M,dCTP})$. The smaller the value of f_{ins}, the more accurate the polymerase. The kinetic values were determined and are reported as in Table 3. [b]The dCTP:dG reactions in Mn^{2+} were performed twice. The mean ± s.e.m. is reported (n = 2).

Table 5. Steady-State Kinetic Parameters for Single Base Insertion on Different Template Bases in the Presence of Manganese

template base	dNTP	k_{cat} (min^{-1})	K_m (mM)	k_{cat}/K_m (min^{-1} mM^{-1})	f_{ins}[a] (misinsertion frequency)
dT	dATP	6.2 ± 0.1	0.015 ± 0.001	410	
	dGTP	0.021 ± 0.001	0.032 ± 0.005	0.66	0.002
dA	dTTP	12.0 ± 0.2	0.045 ± 0.003	270	
	dGTP	0.0053 ± 0.0002	0.017 ± 0.003	0.31	0.001
dC	dGTP	5.6 ± 0.1	0.012 ± 0.001	470	
	dATP	0.013 ± 0.001	0.064 ± 0.012	0.20	0.0004

[a]The frequencies of misinsertion were calculated relative to insertion of dCTP opposite dG using the ratio $(k_{cat}/K_{M,mispaired\ dNTP})/(k_{cat}/K_{M,dCTP})$. The smaller the value of f_{ins}, the more accurate the polymerase. The kinetic values were determined and are reported as in Table 3.

correct nucleotide opposite the four normal template bases. Comparing the efficiencies for accurate insertion events, PrimPol copies template dC > dT > dG > dA, when Mn^{2+} is the cofactor (Tables 4 and 5). Changing the metal ion cofactor to Mg^{2+} does not alter the efficiency of accurate nucleotide insertion (Tables 4 and S2). The absolute specificity constant values describing PrimPol activity ranged from a low of 0.25 mM^{-1} min^{-1} for dAMP:dT to a high of 1.3 mM^{-1} min^{-1} for dGMP:dC in the presence of Mg^{2+}. With Mn^{2+} as the cofactor, the specificity constants ranged from a low of 270 mM^{-1} min^{-1} for dAMP:dT to a high of 470 mM^{-1} min^{-1} for dGMP:dC. There is an approximate 5-fold range in catalytic efficiency for copying the four template bases in Mg^{2+}, compared to only a ~2-fold range in the efficiency of nucleotidyl transfer with Mn^{2+} as the cofactor. We also noted that PrimPol activity on substrates with template dA was stimulated over 1000-fold by Mn^{2+} (Table 5 and Table S2), which is even greater than that observed for substrates with template dG.

Once we had determined the efficiency of accurate DNA synthesis by PrimPol, we then measured the efficiency of misinsertion on undamaged template bases. Prior to performing steady-state kinetics for misinsertion, we performed a short time course for misinsertion on p/t-DNA substrates with either dG or dT as the template base. For both substrates we found that, next to accurate Watson−Crick bp formation, the most efficient misinsertion product was generated when the enzyme is incubated with the dNTP capable of base pairing with the template base at the +1 position (i.e., the dNTP capable of pairing with the template base on the 5′ side of the 0 position to generate −1 frameshift deletion products; data not shown). The steady-state kinetic parameters describing PrimPol-catalyzed misinsertion of dGMP across from template dA, dG, and dT was then measured. We also measured PrimPol-catalyzed misinsertion of dAMP opposite template dC using a slightly altered template sequence. Comparing the fidelity for the four template bases, the misinsertion frequency in the presence of Mn^{2+} was highest (i.e., most error-prone) for template dG (f_{ins} = 0.01) and lowest (i.e., most accurate) for template dC (f_{ins} = 0.0004) (Tables 4 and 5). Steady-state kinetic parameters revealed that PrimPol fidelity is decreased ~1.7-fold by Mn^{2+} when copying template dG, as indicated by an increase in the misinsertion frequency relative to Mg^{2+} (Table 4). These results show that, like other TLS pols, PrimPol makes a mistake copying undamaged template DNA about once every 100−2500 insertion events.

Metal Ion-Dependent Primpol Polymerase Extension Activity on 8-oxo-dG DNA template. PrimPol has been shown to bypass certain DNA adducts, including 8-oxo-dG, 6-4 photoproducts, cyclobutane pyrimidine dimers (CPDs), and tetrahydrofuran (THF) abasic site mimics. The bypass of CPD lesions has only been observed when the zinc finger domain of PrimPol is deleted from the protein.[9] Of these adducts, 8-oxo-dG and abasic sites are of particular importance to replication of mitochondrial DNA since the ratio of 8-oxo-dG to dG in mtDNA is several times higher than in nuclear DNA, and oxidative damage can lead to the formation of abasic sites in mtDNA.[16]

To provide an initial measure for PrimPol-catalyzed bypass of 8-oxo-dG, we compared PrimPol extension activity in the presence of either Mg^{2+} or Mn^{2+} using p/t-DNA substrates containing either template dG or 8-oxo-dG at the insertion point (i.e., standing start extension assays). PrimPol exhibits robust extension activity on both DNA substrates in the presence of Mn^{2+} (Figure 2). There is a slight reduction in the amount of extended product for 8-oxo-dG templates, and there are clearly two products formed when PrimPol copies 8-oxo-dG (Figure 2), presumably due to insertion of either dCMP or dAMP opposite the lesion. The faster migrating of the two bands is more intense than the upper band for both metals and is likely the dCMP insertion product. The ratio of the two bands is slightly different when comparing Mg^{2+} and Mn^{2+}, with the lower band dominating the products when Mg^{2+} is used for the reaction. It is apparent from these experiments that extension by PrimPol is not greatly impeded by 8-oxo-dG and that it is likely inserting both dCMP and dAMP opposite the lesion.

PrimPol Prefers to Insert dCMP Opposite 8-oxo-dG. We next performed steady-state kinetic analysis of PrimPol-

dx.doi.org/10.1021/bi501024u | Biochemistry 2014, 53, 6584−6594

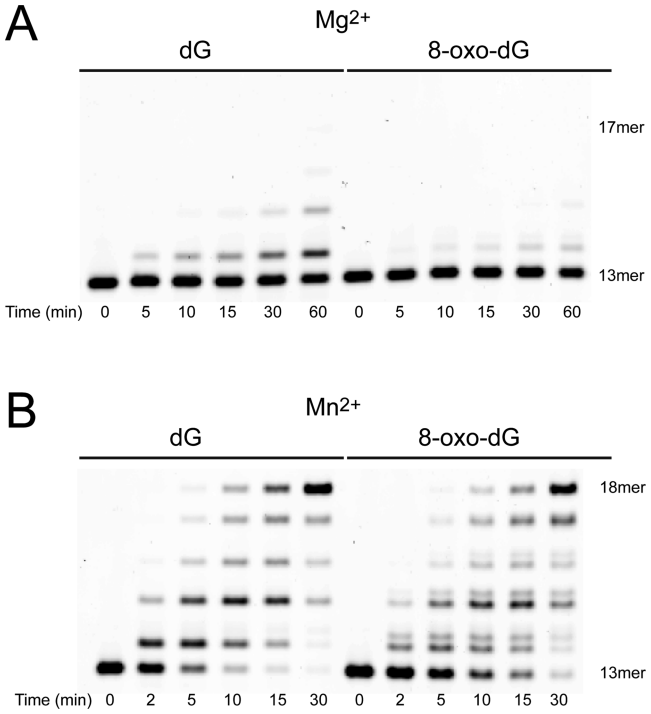

Figure 2. Primer extension by PrimPol on unmodified and 8-oxo-dG-modified DNA templates is increased by manganese. Primpol (250 nM) was incubated with 13/18-mer p/t-DNA (2.5 μM), a mixture of all four dNTPs (250 μM each) and 10 mM of either (A) $MgCl_2$ or (B) $MnCl_2$. The first template base is indicated above the gel (dG or 8-oxo-dG). Primer extension was allowed to proceed for up to 60 and 30 min for Mg^{2+} and Mn^{2+} reactions, respectively, and the products were separated by 16% (w/v) polyacrylamide/7 M urea gel electrophoresis. The inclusion of Mn^{2+} has a pronounced stimulatory effect on DNA synthesis by PrimPol.

catalyzed single-nucleotide insertion of either dCMP or dAMP opposite 8-oxo-dG. PrimPol prefers to insert dCMP opposite 8-oxo-dG over dAMP misinsertion based on steady-state kinetic parameters (Table 6). PrimPol catalytic efficiency, as measured by changes in the specificity constant, is decreased to 26% during insertion of dCMP opposite 8-oxo-dG (relative to dCMP insertion opposite dG). The fidelity of PrimPol-catalyzed insertion opposite 8-oxo-dG is affected somewhat by the identity of the metal ion cofactor. Insertion of dCMP opposite 8-oxo-dG is 5.7-fold more efficient than dAMP misinsertion when Mg^{2+} is the cofactor and only 1.8-fold when Mn^{2+} is the cofactor. Thus, PrimPol-catalyzed bypass of 8-oxo-dG is 3.2-fold less accurate in Mn^{2+} than it is in Mg^{2+}. The metal ion-dependent decrease in fidelity for 8-oxo-dG bypass (3.2-fold) is slightly greater than the metal ion-dependent change in fidelity observed for undamaged template DNA (1.7-fold). Nevertheless, these results lead us to conclude that PrimPol prefers to catalyze accurate bypass of 8-oxo-dG, regardless of whether Mn^{2+} or Mg^{2+} is used.

PrimPol Prefers to Extend From dC:8-oxo-dG Base Pairs over dA:8-oxo-dG Mispairs. From our pol extension gels, it was obvious that PrimPol readily extends past 8-oxo-dG sites (Figure 2). Our single-nucleotide results revealed that accurate insertion opposite the lesion is preferred, but it remained to be seen if PrimPol preferentially extends from dC:8-oxo-dG or dA:8-oxo-dG pairs. In order to determine PrimPol fidelity at the extension step past 8-oxo-dG, we measured the catalytic efficiency of PrimPol-catalyzed next-base extension from primers containing either dC or dA paired opposite dG and 8-oxo-dG (substrates 11−14). We first measured next-base extension for unmodified DNA substrates and found that PrimPol extends from dC:dG bps ~2500-fold more efficiently than dA:dG mispairs (Table 7). As with the insertion step, PrimPol shows a preference for accurate bypass of 8-oxo-dG, extending from dC:8-oxo-dG bp 1.8- (Mg^{2+}) to 2.1-fold (Mn^{2+}) better than dA:8-oxo-dG mispairs (Table 7). The efficiency of the next-base extension step past dC:8-oxo-dG bps increases back to near the level observed for unmodified DNA templates (~75% to 85% of that observed for undamaged DNA), which is consistent with a mild reduction in PrimPol DNA synthesis in extending past 8-oxo-dG lesions.

PrimPol Either Skips Over or Uses the "A-rule" To Copy the THF Abasic Site Mimic. Compared to nucleotide insertion opposite 8-oxo-dG, PrimPol exhibits weak catalytic proficiency on a THF containing template, preferentially skipping over the lesion and inserting dGMP opposite template dC positioned just 5′ of THF (Table 8). The specificity constant for dGMP insertion on the THF substrate is ~0.04% of that measured for dGMP insertion opposite template dC, and dAMP insertion on the THF substrate is ~0.03% of that observed for dATP insertion opposite template dT. The slight preference for skipping past the THF moiety is driven primarily by a larger increase in the Michaelis constant for dAMP insertion relative to what is observed for dGMP (Table 8). Thus, PrimPol is more strongly impaired by the THF abasic mimic than 8-oxo-dG, and it shows nearly equal preference for either skipping past the abasic site or inserting dAMP.

DISCUSSION

Cellular responses to perturbed replication involve the coordination of many different proteins and enzymes.[17] The discovery of PrimPol as a component of nuclear and mitochondrial DNA replication has led to new models for translesion synthesis and replication fork restart. PrimPol and replication protein A (RPA) colocalize to foci in 293T cells following exposure to hydroxyurea and ionizing radiation.[5] There is also a reported role for PrimPol in the bypass of UV irradiation induced DNA damage.[10,11] The proposed role of PrimPol in mitochondrial DNA replication is especially exciting

Table 6. Steady-State Kinetic Parameters for Single Nucleotide Insertion Opposite 8-oxo-dG[a]

lesion	metal	dNTP	k_{cat} (min^{-1})	K_m (mM)	k_{cat}/K_m (min^{-1} mM^{-1})
8-oxo-dG	Mg^{2+}	dCTP	0.23 ± 0.02	1.4 ± 0.3	0.17
		dATP	0.04 ± 0.003	1.2 ± 0.3	0.03
8-oxo-dG	Mn^{2+}	dCTP	4.0 ± 0.2	0.052 ± 0.008	77
		dATP	2.2 ± 0.1	0.052 ± 0.013	42

[a]The kinetic values were determined and are reported as in Table 3.

dx.doi.org/10.1021/bi501024u | Biochemistry 2014, 53, 6584−6594

Table 7. Steady-State Kinetic Parameters for Next-Base Extension in the Presence of Magnesium and Manganese

template[a]	dNTP	metal	k_{cat} (min^{-1})	K_m (mM)	k_{cat}/K_m (min^{-1} mM^{-1})
5′—CC –3′ 3′—GG<u>C</u>—5′	dGTP	Mg^{2+}	0.50 ± 0.04	0.98 ± 0.23	0.51
		Mn^{2+}	5.4 ± 0.1	0.020 ± 0.002	270
5′—CC -3′ 3′—GX<u>C</u>—5′	dGTP	Mg^{2+}	0.48 ± 0.01	1.2 ± 0.1	0.39
		Mn^{2+}	6.9 ± 0.3	0.030 ± 0.006	230
5′—CA -3′ 3′—GG<u>C</u>—5′	dGTP	Mg^{2+}	0.00021 ± 0.00005	1.1 ± 0.7	0.00019
		Mn^{2+}	0.0026 ± 0.0003	0.024 ± 0.01	0.11
5′—CA -3′ 3′—GX<u>C</u>—5′	dGTP	Mg^{2+}	0.20 ± 0.01	0.91 ± 0.12	0.22
		Mn^{2+}	3.4 ± 0.1	0.031 ± 0.005	110

[a]X represents 8-oxo-dG lesion. The template dC paired with the incoming dGTP is underlined. The kinetic values were determined and are reported as in Table 3.

Table 8. Steady-State Kinetic Parameters for Single Nucleotide Insertion Opposite a THF Abasic Site Mimic[a]

lesion	metal	dNTP	k_{cat} (min^{-1})	K_m (mM)	k_{cat}/K_m (min^{-1} mM^{-1})
abasic	Mn^{2+}	dATP	0.012 ± 0.007	0.11 ± 0.02	0.11
		dGTP	0.0085 ± 0.0002	0.048 ± 0.005	0.18

[a]The kinetic values were determined and are reported as in Table 3.

because of the dearth of translesion synthesis and DNA repair elements known to function in the mitochondria. A number of recent papers have reported on several biochemical and biological aspects of human PrimPol activity, but kinetic analysis of this new enzyme has yet to be investigated. We sought to determine some of the kinetic parameters describing human PrimPol activity in order to better understand how it compares to other TLS and DNA repair pols and gauge its potential contributions to DNA replication at sites of damage.

First, both Mn^{2+} and the length of the ssDNA overhang increase the affinity of PrimPol for p/t-DNA (Table 2). Our results also show that PrimPol has a ∼16-fold preference for utilizing Mn^{2+} over Mg^{2+} during DNA synthesis (Table 3). Furthermore, we find that the specificity constant for nucleotide insertion is increased 400−1000-fold by Mn^{2+} relative to Mg^{2+} (Tables 4 and 5). The metal ion-dependent change in fidelity is not large for unmodified DNA (∼1.7-fold). Importantly, the misinsertion frequency of PrimPol on normal template DNA ranged from one mistake every 100−2500 catalytic events, which is comparable to other TLS pols like the Y-family members.[18]

Others have shown that PrimPol can copy past 8-oxo-dG lesions with relatively little pausing.[4] However, it was unclear how accurate PrimPol was based on the qualitative experiments with 8-oxo-dG. The misinsertion of dAMP opposite 8-oxo-dG is the most common mistake made by pols, due in large part to the thermodynamically favorable pairing betweein *syn* oriented 8-oxo-dG and the incoming dATP.[19,20] Also, the (*syn*) 8-oxo-dG: (*anti*) dA base pair is geometrically deceptive to DNA pols due to its similarity to dT:dA bps. If we take into account both the insertion and the extension steps, then accurate bypass of 8-oxo-dG by PrimPol is around 4- (Mn^{2+}) to 10-fold (Mg^{2+}) more efficient than misinsertion based on steady-state measurements. The ability of PrimPol to catalyze effective and accurate bypass of 8-oxo-dG is likely important for assisting both hpol γ, as well as POLRMT, both of which are impeded by this ubiquitous DNA adduct. Since hpol γ is the main mitochondrial DNA pol, it will undoubtedly encounter 8-oxo-dG lesions that have not been removed by BER. Kinetic studies have shown that the transient state specificity constant for hpol γ-catalyzed insertion of dCMP opposite 8-oxo-dG is decreased ∼470-fold relative to template dG.[21] As it turns out, hpol γ-catalyzed bypass of the lesion is accurate ∼90% of the time, but the fidelity of the enzyme is diminished ∼30000-fold.[21] In this respect, PrimPol could provide the mitochondria with a relatively accurate means of copying 8-oxo-dG with only a moderate decrease in catalytic efficiency.

The fact that PrimPol can catalyze bypass of 8-oxo-dG in a relatively accurate fashion is interesting, though it is not the only enzyme capable of accurately bypassing 8-oxo-dG. Human pol λ appears to be among the most accurate DNA pols at copying 8-oxo-dG.[22] Human and yeast pol η also prefer to insert dCMP opposite 8-oxo-dG.[23,24] The Y-family member, hpol κ, is quite error-prone, preferring dAMP insertion ∼10-fold more than accurate insertion of dCMP.[19,25] A previous report on PrimPol erroneously stated that addition of PCNA and RPA stimulated pols λ and η to perform misinsertion of dAMP opposite 8-oxo-dG.[9] This statement is not correct. Adding accessory factors, such as PCNA and RPA, increases the fidelity of translesion synthesis opposite 8-oxo-dG by stimulating accurate insertion of dCMP opposite the lesion. In the presence of RPA and PCNA, DNA pol λ incorporates dCMP 1200-fold more effectively than misinsertion of dAMP opposite 8-oxoG and hpol η performs accurate insertion of dCMP 68-fold better than dAMP opposite the adduct.[22] It remains to be seen if RPA can stimulate PrimPol action on 8-oxo-dG, but it seems unlikely that it will achieve the levels of accuracy reported for either pols λ or η.

Compared to other TLS pols, PrimPol insertion across from the THF modification is not effective, with ∼10^3-fold reduction in the specificity constant. This decrease in PrimPol activity is ∼10-fold greater than that observed for Dpo4 from *Sulfolobus solfataricus*.[26,27] PrimPol is also not nearly as effective as either hpol η, hpol ι, or hRev1 at bypassing abasic sites.[28] The contribution of PrimPol to abasic site replication in cells

dx.doi.org/10.1021/bi501024u | *Biochemistry* 2014, 53, 6584−6594

remains uncertain, but it appears to be inhibited substantially by these lesions based on our kinetic results.

Sequence comparisons have revealed that human PrimPol belongs to an ancient class of enzymes that function to replicate small DNA genomes. PrimPol shows sequence similarity to archaeal and eukaryotic primases, and it contains a zinc finger homologous to that of herpesvirus UL52 primase.[4] On the basis of sequence homology, PrimPol may share structural features with a bifunctional primase-polymerase enzyme ORF904 encoded by the pRN1 plasmid from *Sulfolobus islandicus*. The pRN1-derived ORF904 primpol crystal structure has been solved, revealing that a catalytic triad (Asp^{111}, Glu^{113}, and Asp^{171}) is responsible for both the primase and the pol activities of this bifunctional enzyme.[29] It would seem that PrimPol also has a single catalytic site since mutation of Asp^{114} and Glu^{116} abolishes both primase and pol activities of the enzyme.[4] The ORF904 primpol crystal structure reveals a shallower DNA binding surface than other DNA pols.[29] It has been postulated that the zinc finger domain of PrimPol may act in a manner similar to the little finger or polymerase-associated domain (PAD) of the Y-family pols.[9] Comparing the structure of ORF904 prim-pol to Y-family pols (Figure S1), it seems more likely that the zinc stem is positioned in a manner that is analogous to the finger domain of Y-family pols, while the so-called "DNA-binding sub-domain" (a.a. 1−100 in ORF904) is acting in a fashion comparable to the little finger domain. In a general sense, the secondary structural elements of the ORF904 DNA-binding subdomain represent a compressed or miniaturized version of the Y-family little finger domain, with three short beta sheets set atop two alpha helices and facing the proposed DNA binding site (Figure S1). The little finger structure for Y-family pols is composed of four beta sheets lining the DNA binding cleft and backed by two alpha helices. In this way, the overall arrangement of the ORF904 domain architecture (and by inference, the structure of PrimPol) may not be all that dissimilar to other TLS pols.

In terms of metal ion utilization by PrimPol, the decrease in the $K_{d,DNA}$ and the increase in the k_{cat} for Mn^{2+} relative to Mg^{2+} are what drives the preference for Mn^{2+} (Table 3). The 400−1000-fold increase in the value for the specificity constant describing dNMP insertion in the presence of Mn^{2+} stems from a large increase in the k_{cat} and an equally large decrease in the $K_{m,dNTP}$ (Tables 4, 5, and S2). Mechanistically speaking, we cannot say if the decrease in the $K_{m,dNTP}$ is due to a higher affinity for the incoming dNTP, but this would seem to be a reasonable possibility. Transient-state kinetic analysis of PrimPol activity is ongoing and will likely provide greater insight into how Mn^{2+} affects individual steps within the catalytic cycle of PrimPol. However, it is clear that the $K_{M,dNTP}$ values measured for PrimPol-catalyzed primer extension are very high (in the hundreds of micromolar), to the point where one could postulate that the DNA pol activity of PrimPol would not function in cells (where the concentration of the dNTP pool is in the tens of micromolar) unless Mn^{2+} is bound in the active site of the enzyme. This scenario seems even more likely in the mitochondria where dNTP levels are about an order of magnitude lower than those in the cytosol.[30]

Other TLS pols have been shown to exhibit higher catalytic proficiency in the presence of Mn^{2+}. For example, the catalytic efficiency of Dpo4 from *Sulfolobus solfataricus* is increased ∼3-fold by Mn^{2+} on unmodified DNA templates and ∼10-fold on substrates containing either THF or CPD lesions.[31] Dpo4 fidelity on unmodified DNA templates is decreased 4.3-fold by Mn^{2+}.[31] The catalytic activity of hpol ι is stimulated ∼1600-fold by Mn^{2+} on undamaged DNA and ∼2000-fold on substrates containing N^2-ethyl-dG,[32] which is greater than what we observe with PrimPol. However, like PrimPol, hpol ι shows modest decreases in fidelity in the presence of Mn^{2+}.[33] Hpol κ, on the other hand, shows diminished catalytic efficiency for Mn^{2+} compared to Mg^{2+}.[33] Even more striking is the large decrease in hpol κ fidelity observed when Mn^{2+} is substituted for Mg^{2+}. Steady-state kinetic parameters indicate that nucleotide selection by hpol κ is ∼6000-fold less faithful in the presence of Mn^{2+}.[33] The Mn^{2+}-dependent changes in hpol κ activity and fidelity are reminiscent of those observed for replicative pols. Finally, studies with the X-family members pols β, λ, and μ have shown that each of these enzymes preferentially utilize Mn^{2+} over Mg^{2+}, with differing effects upon fidelity.[34−36]

It was established decades ago that Mn^{2+} could induce mutagenic DNA synthesis in manner that seems to affect mitochondria more than nuclear components, and it has long been recognized that DNA pols are generally more error-prone in the presence of Mn^{2+}.[34−36] Structural comparisons between Mg^{2+} and Mn^{2+} coordinated in the active site of Dpo4 reveals that relaxed coordination requirements for Mn^{2+} contribute to error-prone synthesis by allowing a greater range of productive base pair arrangements.[31] While the exact biological relevance of Mn^{2+} toward mtDNA replication is unclear, it is interesting to note the relatively large >400-fold activation of PrimPol catalysis that accompanies substituting Mg^{2+} with Mn^{2+}, given the reported role for PrimPol in mtDNA replication. Still, it is not clear if physiological concentrations of Mn^{2+} are sufficient to compete with Mg^{2+} for pol active sites. The concentration of intracellular Mg^{2+} ranges from 14 mM to 20 mM in mammalian cells with considerably less free Mg^{2+} in the cytosol (∼0.5−0.7 mM).[37] Intracellular Mn^{2+} has been measured near 10 μM.[38] In the last several years, a newly identified class of ion transporters called natural resistance-associated macrophage proteins (NRAMPs) have been shown to regulate Mn^{2+} concentrations in the cell.[39] These NRAMP proteins have been identified in prokaryotes and eukaryotes, including humans. NRAMP-mediated ion transport can increase intracellular Mn^{2+} concentrations to >300 μM.[39] In bacteria, NRAMP proteins are up-regulated in response to treatment with hydrogen peroxide, which leads to the intriguing possibility that an influx of Mn^{2+} could activate PrimPol (and perhaps other TLS pols) during periods when oxidative damage to DNA is increased. However, it is also possible that the utilization of Mg^{2+} by PrimPol leads to incorporation of only a single nucleotide, which could be sufficient for bypass of DNA damage and thereby limit the risk of PrimPol-induced mutagenesis.

The ability of PrimPol to accurately bypass 8-oxo-dG during periods of oxidative stress could impact human health by preventing the untimely depletion of mtDNA. The role of mitochondrial DNA replication components in human disease is well documented. Mutations in the *POLG* gene, encoding the catalytic subunit of hpol γ, are heterogeneous and result in multiple disorders, such as progressive external ophthalmoplegia, parkinsonism, premature menopause, and Alpers syndrome.[40] Interestingly, a recent exome sequencing study identified missense mutations in the *CCDC111* gene that encodes PrimPol in a family diagnosed with high myopia.[41] The resulting Y89D amino acid change in PrimPol occurs in a position that is highly conserved across species (from humans through zebrafish) and is predicted to reside in the DNA-

binding subdomain of human PrimPol at a residue that may be homologous to Phe[88] in ORF904 primpol from *S. islandicus*, based on sequence comparisons. The structure of ORF904 primpol shows Phe[88] to reside in the α2 helix, which sits on the opposite face of the subdomain that is predicted to be in contact with DNA.[29] When considering the potential impact of the Y89D change observed for human PrimPol, it is possible that changing Tyr to Asp could be slightly more disruptive to α-helix formation, but it could also result in altered interactions with RNA/DNA. Future studies will investigate the functional changes to PrimPol action that are imposed by the Y89D mutation.

In summary, we have performed the first in depth kinetic analysis of the DNA pol activity of human PrimPol. We find that PrimPol preferentially binds to p/t-DNA with longer ssDNA overhangs and that binding is tighter when Mn^{2+} is the cofactor. The polymerization activity of PrimPol is strongly stimulated by Mn^{2+}. We quantified the PrimPol misinsertion frequency on undamaged DNA templates and find that the fidelity of polymerization is indeed comparable to other TLS pols (1 mistake every ~100−2500 insertion events). Finally, we provide evidence that PrimPol prefers to bypass 8-oxo-dG in an accurate manner, clarifying previous qualitative suggestions to the contrary. The mechanism by which PrimPol is recruited to sites of stalled mitochondrial DNA replication and/or transcription by POLRMT is still an active area of investigation, and additional studies are needed to decipher the exact role of PrimPol in the maintenance of mtDNA.

■ ASSOCIATED CONTENT

Supporting Information

Supporting Tables S1 and S2 report on ssDNA binding and steady-state kinetic parameters describing PrimPol activity in magnesium, and Figure S1 compares structural elements of ORF904 primpol from *Sulfolobus islandicus* and Dpo4 from *Sulfolobus solfataricus*. This material is available free of charge via the Internet at http://pubs.acs.org.

■ AUTHOR INFORMATION

Corresponding Author

*E-mail: rleoff@uams.edu. Telephone: 501-686-8343. Fax: 501-686-8169.

Funding

This work was supported in part by U.S.P.H. service grants from the National Institutes of Health (CA183895 to R.L.E. and AI045818 to C.E.C.) with additional support from the University of Arkansas for Medical Sciences Translational Research Institute (CTSA Grant Award UL1TR000039). Funding for open access charge: The University of Arkansas for Medical Sciences, College of Medicine.

Notes

The authors declare no competing financial interest.

■ ACKNOWLEDGMENTS

We thank Dr. Matthew Pence for critically reading our manuscript and for helpful suggestions.

■ ABBREVIATIONS

8-oxo-dG, 7,8-dihydro-8-oxo-2′-deoxyguanosine; dNTPs, deoxyribonucleotide triphosphates; DTT, dithiothreitol; EDTA, ethylenediaminetetraacetic acid; POLRMT, mitochondrial RNA polymerase; pol, polymerase; THF, tetrahydrofuran; TLS, translesion DNA synthesis

■ REFERENCES

(1) Friedberg, E. C., Lehmann, A. R., and Fuchs, R. P. (2005) Trading places: how do DNA polymerases switch during translesion DNA synthesis? *Mol. Cell 18*, 499−505.

(2) Kunkel, T. A., and Burgers, P. M. (2008) Dividing the workload at a eukaryotic replication fork. *Trends Cell Biol. 18*, 521−527.

(3) Langston, L. D., Indiani, C., and O'Donnell, M. (2009) Whither the replisome: emerging perspectives on the dynamic nature of the DNA replication machinery. *Cell Cycle 8*, 2686−2691.

(4) Garcia-Gomez, S., Reyes, A., Martinez-Jimenez, M. I., Chocron, E. S., Mouron, S., Terrados, G., Powell, C., Salido, E., Mendez, J., Holt, I. J., and Blanco, L. (2013) PrimPol, an archaic primase/polymerase operating in human cells. *Mol. Cell 52*, 541−553.

(5) Wan, L., Lou, J., Xia, Y., Su, B., Liu, T., Cui, J., Sun, Y., Lou, H., and Huang, J. (2013) hPrimpol1/CCDC111 is a human DNA primase-polymerase required for the maintenance of genome integrity. *EMBO Rep. 14*, 1104−1112.

(6) Iyer, L. M., Koonin, E. V., Leipe, D. D., and Aravind, L. (2005) Origin and evolution of the archaeo-eukaryotic primase superfamily and related palm-domain proteins: structural insights and new members. *Nucleic Acids Res. 33*, 3875−3896.

(7) Cloutier, S., Hamel, H., Champagne, M., and Yotov, W. V. (1997) Mapping of the human DNA primase 1 (PRIM1) to chromosome 12q13. *Genomics 43*, 398−401.

(8) Stadlbauer, F., Brueckner, A., Rehfuess, C., Eckerskorn, C., Lottspeich, F., Förster, V., Tseng, B. Y., and Nasheuer, H.-P. (1994) DNA replication *in vitro* by recombinant DNA-polymerase-α-primase. *Eur. J. Biochem. 222*, 781−793.

(9) Keen, B. A., Jozwiakowski, S. K., Bailey, L. J., Bianchi, J., and Doherty, A. J. (2014) Molecular dissection of the domain architecture and catalytic activities of human PrimPol. *Nucleic Acids Res. 42*, 5830−5845.

(10) Mouron, S., Rodriguez-Acebes, S., Martinez-Jimenez, M. I., Garcia-Gomez, S., Chocron, S., Blanco, L., and Mendez, J. (2013) Repriming of DNA synthesis at stalled replication forks by human PrimPol. *Nat. Struct. Mol. Biol. 20*, 1383−1389.

(11) Bianchi, J., Rudd, S. G., Jozwiakowski, S. K., Bailey, L. J., Soura, V., Taylor, E., Stevanovic, I., Green, A. J., Stracker, T. H., Lindsay, H. D., and Doherty, A. J. (2013) PrimPol bypasses UV photoproducts during eukaryotic chromosomal DNA replication. *Mol. Cell 52*, 566−573.

(12) Wong, T. W., and Clayton, D. A. (1985) Isolation and characterization of a DNA primase from human mitochondria. *J. Biol. Chem. 260*, 11530−11535.

(13) Chang, D. J., and Cimprich, K. A. (2009) DNA damage tolerance: when it's OK to make mistakes. *Nat. Chem. Biol. 5*, 82−90.

(14) Cortez, D. (2005) Unwind and slow down: checkpoint activation by helicase and polymerase uncoupling. *Genes Dev. 19*, 1007−1012.

(15) Maddukuri, L., Ketkar, A., Eddy, S., Zafar, M. K., Griffin, W. C., and Eoff, R. L. (2012) Enhancement of human DNA polymerase η activity and fidelity is dependent upon a bipartite interaction with the Werner's syndrome protein. *J. Biol. Chem. 287*, 42312−42323.

(16) Richter, C., Park, J. W., and Ames, B. N. (1988) Normal oxidative damage to mitochondrial and nuclear DNA is extensive. *Proc. Natl. Acad. Sci. U. S. A. 85*, 6465−6467.

(17) Osborn, A. J., Elledge, S. J., and Zou, L. (2002) Checking on the fork: the DNA-replication stress-response pathway. *Trends Cell Biol. 12*, 509−516.

(18) Kunkel, T. A. (2004) DNA replication fidelity. *J. Biol. Chem. 279*, 16895−16898.

(19) Irimia, A., Eoff, R. L., Guengerich, F. P., and Egli, M. (2009) Structural and functional elucidation of the mechanism promoting error-prone synthesis by human DNA polymerase kappa opposite the 7,8-dihydro-8-oxo-2′-deoxyguanosine adduct. *J. Biol. Chem. 284*, 22467−22480.

(20) McAuley-Hecht, K. E., Leonard, G. A., Gibson, N. J., Thomson, J. B., Watson, W. P., Hunter, W. N., and Brown, T. (1994) Crystal structure of a DNA duplex containing 8-hydroxydeoxyguanine-adenine base pairs. *Biochemistry 33*, 10266−10270.
(21) Hanes, J. W., Thal, D. M., and Johnson, K. A. (2006) Incorporation and replication of 8-oxo-deoxyguanosine by the human mitochondrial DNA polymerase. *J. Biol. Chem. 281*, 36241−36248.
(22) Maga, G., Villani, G., Crespan, E., Wimmer, U., Ferrari, E., Bertocci, B., and Hubscher, U. (2007) 8-oxo-guanine bypass by human DNA polymerases in the presence of auxiliary proteins. *Nature 447*, 606−608.
(23) Haracska, L., Yu, S. L., Johnson, R. E., Prakash, L., and Prakash, S. (2000) Efficient and accurate replication in the presence of 7,8-dihydro-8-oxoguanine by DNA polymerase eta. *Nat. Genet. 25*, 458−461.
(24) Patra, A., Nagy, L. D., Qianqian, Z., Su, Y., Müller, L., Guengerich, F. P., and Egli, M. (2014) Kinetics, structure, and mechanism of 8-oxo-7,8-dihydro-2′-deoxyguanosine bypass by human DNA polymerase *η*. *J. Biol. Chem. 289*, 16867−16882.
(25) Haracska, L., Prakash, L., and Prakash, S. (2002) Role of human DNA polymerase kappa as an extender in translesion synthesis. *Proc. Natl. Acad. Sci. U. S. A. 99*, 16000−16005.
(26) Fiala, K. A., Hypes, C. D., and Suo, Z. (2007) Mechanism of abasic lesion bypass catalyzed by a Y-family DNA polymerase. *J. Biol. Chem. 282*, 8188−8198.
(27) Fiala, K. A., and Suo, Z. (2007) Sloppy bypass of an abasic lesion catalyzed by a Y-family DNA polymerase. *J. Biol. Chem. 282*, 8199−8206.
(28) Choi, J. Y., Lim, S., Kim, E. J., Jo, A., and Guengerich, F. P. (2010) Translesion synthesis across abasic lesions by human B-family and Y-family DNA polymerases *α*, *δ*, *η*, *ι*, *κ*, and REV1. *J. Mol. Biol. 404*, 34−44.
(29) Lipps, G., Weinzierl, A. O., von Scheven, G., Buchen, C., and Cramer, P. (2004) Structure of a bifunctional DNA primase-polymerase. *Nat. Struct. Mol. Biol. 11*, 157−162.
(30) Rampazzo, C., Ferraro, P., Pontarin, G., Fabris, S., Reichard, P., and Bianchi, V. (2004) Mitochondrial deoxyribonucleotides, pool sizes, synthesis, and regulation. *J. Biol. Chem. 279*, 17019−17026.
(31) Vaisman, A., Ling, H., Woodgate, R., and Yang, W. (2005) Fidelity of Dpo4: effect of metal ions, nucleotide selection and pyrophosphorolysis. *EMBO J. 24*, 2957−2967.
(32) Pence, M. G., Blans, P., Zink, C. N., Hollis, T., Fishbein, J. C., and Perrino, F. W. (2009) Lesion bypass of N^2-ethylguanine by human DNA polymerase iota. *J. Biol. Chem. 284*, 1732−1740.
(33) Pence, M. G., Blans, P., Zink, C. N., Fishbein, J. C., and Perrino, F. W. (2010) Bypass of N(2)-ethylguanine by human DNA polymerase kappa. *DNA Repair (Amst) 10*, 56−64.
(34) Goodman, M. F., Keener, S., Guidotti, S., and Branscomb, E. W. (1983) On the enzymatic basis for mutagenesis by manganese. *J. Biol. Chem. 258*, 3469−3475.
(35) Kunkel, T. A., and Loeb, L. A. (1979) Effect of divalent metal ion activators and deoxyribonucleoside triphosphate pools on *in vitro* mutagenesis. *J. Biol. Chem. 254*, 5718−5725.
(36) Putrament, A., Baranokowska, A. E., and Prazmo, W. (1975) Manganese mutagenesis in yeast. A practical application of manganese for the induction of mitochondrial antibiolitc-resistant mutations. *J. Gen. Microbiol. 62*, 265−270.
(37) Romani, A. (2007) A magnificent story in the making. *Arch. Biochem. Biophys. 458*, 90−102.
(38) Kehres, D. G., and Maguire, M. E. (2003) Emerging themes in manganese transport, biochemistry and pathogenesis in bacteria. *FEMS Microbiol. Rev. 27*, 263−290.
(39) Kehres, D. G., Zaharik, M. L., Finlay, B. B., and Maguire, M. E. (2000) The NRAMP proteins of *Salmonella typhimurium* and *Escherichia coli* are selective manganese transporters involved in the response to reactive oxygen. *Mol. Microbiol. 36*, 1085−1100.
(40) Copeland, W. C. (2008) Inherited mitochondrial diseases of DNA replication. *Annu. Rev. Med. 59*, 131−146.
(41) Zhao, F., Wu, J., Xue, A., Su, Y., Wang, X., Lu, X., Zhou, Z., Qu, J., and Zhou, X. (2013) Exome sequencing reveals CCDC111 mutation associated with high myopia. *Hum. Genet. 132*, 913−921.